

**$N = 82$  Shell Quenching of the Classical  $r$ -Process “Waiting-Point” Nucleus  $^{130}\text{Cd}$** I. Dillmann,<sup>1,2</sup> K.-L. Kratz,<sup>1,\*</sup> A. Wöhr,<sup>3,4</sup> O. Arndt,<sup>1</sup> B. A. Brown,<sup>5</sup> P. Hoff,<sup>6</sup> M. Hjorth-Jensen,<sup>7</sup> U. Köster,<sup>8</sup>  
A. N. Ostrowski,<sup>1</sup> B. Pfeiffer,<sup>1</sup> D. Seweryniak,<sup>9</sup> J. Shergur,<sup>3,9</sup> W. B. Walters,<sup>3</sup> and the ISOLDE Collaboration<sup>8</sup><sup>1</sup>*Institut für Kernchemie, Universität Mainz, Mainz, Germany*<sup>2</sup>*Departement für Physik und Astronomie, Universität Basel, Basel, Switzerland*<sup>3</sup>*Department of Chemistry, University of Maryland, College Park, Maryland, USA*<sup>4</sup>*Department of Physics, University of Notre Dame, Notre Dame, Indiana, USA*<sup>5</sup>*Department of Physics and Astronomy and NSCL, Michigan State University, East Lansing, Michigan, USA*<sup>6</sup>*Department of Chemistry, University of Oslo, Oslo, Norway*<sup>7</sup>*Department of Physics, University of Oslo, Oslo, Norway*<sup>8</sup>*CERN, Geneva, Switzerland*<sup>9</sup>*Physics Division, Argonne National Laboratory, Argonne, Illinois, USA*

(Received 28 July 2003; published 16 October 2003)

First  $\beta$ - and  $\gamma$ -spectroscopic decay studies of the  $N = 82$   $r$ -process “waiting-point” nuclide  $^{130}\text{Cd}$  have been performed at CERN/ISOLDE using the highest achievable isotopic selectivity. Several nuclear-physics surprises have been discovered. The first one is the unanticipatedly high energy of 2.12 MeV for the  $[\pi g_{9/2} \otimes \nu g_{7/2}] 1^+$  level in  $^{130}\text{In}$ , which is fed by the main Gamow-Teller transition. The second surprise is the rather high  $Q_\beta$  value of 8.34 MeV, which is in agreement only with recent mass models that include the phenomenon of  $N = 82$  shell quenching. Possible implications of these new results on the formation of the  $A \approx 130$   $r$ -process abundance peak are presented.

DOI: 10.1103/PhysRevLett.91.162503

PACS numbers: 23.20.Lv, 21.10.Dr, 26.30.+k, 27.60.+j

**Introduction.**—The theory of nucleosynthesis predicts that most of the nuclear species beyond Fe are formed as a consequence of two distinct neutron-capture processes, i.e., a *slow* (“ $s$ ”) process with small neutron densities ( $\approx 10^8 \text{ cm}^{-3}$ ) and a *rapid* (“ $r$ ”) process with high neutron densities ( $> 10^{20} \text{ cm}^{-3}$ ). A strong support for this view is provided by the splitting of the peak structure of heavy element solar-system abundances ( $N_\odot$ ), which are correlated with neutron shell closures at  $N = 50, 82,$  and  $126$  [1,2]. Also the early ideas of the “*waiting-point*” concept, that successive neutron capture is limited by photodisintegrations and a “*waiting*” for  $\beta$  decays to take place, are still used in many  $r$ -process calculations.

The classical  $N = 82$   $r$ -process waiting-point isotope  $^{130}\text{Cd}$  was first identified by Kratz *et al.* in 1986 [3] at the SC-ISOLDE at CERN, where a  $\beta$ -decay half-life of  $T_{1/2} = (195 \pm 35)$  ms could be determined from multi-scaling of  $\beta$ -delayed neutrons. This value was in reasonable agreement with the  $N_{r,\odot}(Z) \times \lambda_\beta(Z) \approx \text{constant}$  waiting-point expectation of  $(180 \pm 20)$  ms, derived independently at that time by Hillebrandt and Thielemann [4]. The correlation between the half-life of  $^{130}\text{Cd}$  and the observed solar  $r$  abundance of its stable isobar  $^{130}\text{Te}$  immediately became essential to constrain the equilibrium conditions of an  $r$  process. Following this initial measurement, it took over ten years until the half-life of  $^{129}\text{Ag}$  (46 ms) could be determined, and a more precise value of 162 ms for the  $\beta$  decay of  $^{130}\text{Cd}$  was obtained [5,6]. In the meantime, the availability of these two *measured* half-lives stimulated a number of theoretical attempts to calculate half-lives of the lower- $Z$   $N = 82$  isotones  $^{128}\text{Pd}$  to  $^{122}\text{Zr}$  and to examine the astrophysi-

cal consequences of the various results. For all of these even-even  $N = 82$  waiting-point nuclides, the important nuclear-structure properties are the  $Q_\beta$  value, the location of the  $[\pi g_{9/2} \otimes \nu g_{7/2}]$  two quasiparticle (2QP)  $1^+$  level ( $E^{1+}$ ) in  $^{130}\text{In}$  populated by Gamow-Teller (GT) decay and its log ft value. Thus, because of the interrelationship of these three essential quantities, it is possible to calculate similar half-lives, based on widely different model assumptions [7,8].

In this Letter, we report new measurements for all of these crucial properties for the decay of  $^{130}\text{Cd}$ . We also discuss the implications of our new data for values of the lower- $Z$  isotones and for  $r$ -process nucleosynthesis.

**Experimental procedures.**—Since the first identification of  $^{130}\text{Cd}$ , several technical developments have been necessary to perform new experiments with enhanced selectivity at the ISOLDE facility. In a two-step process, the 1 GeV proton beam from the PS-Booster is impinging on a Ta or a W rod in close proximity to the  $\text{UC}_x\text{-C}$  target, leading the fast reaction neutrons to induce fission. With this “neutron converter” method [9], proton-rich isobaric spallation products (e.g., surface-ionized 29 m  $^{130}\text{Cs}$ ) are suppressed to a large extent.

The second and most important improvement was the development and installation of a resonance-ionization laser ion source (RILIS) to achieve chemical selectivity for elements with high ionization potentials (e.g., Ag, Cd, and Sn). For that purpose, the reaction products are laser ionized after diffusing out of the heated target. With the RILIS, it is possible to run the laser ion source in two different modes. The “*laser off*” mode shows only surface-ionized In, whereas in the “*laser on*” mode we

additionally get laser-ionized Cd. By comparing the respective  $\gamma$  spectra, one can unambiguously identify  $\gamma$  lines corresponding to the  $\beta$  decay of  $^{130}\text{Cd}$ . A further enhancement of selectivity was possible with the use of the “high resolution separator” (HRS). With a mass resolution of  $M/\Delta M \approx 4300$ , the HRS considerably reduced the isobaric In background at  $A = 130$ . More detailed descriptions of the technical setup, the detectors, and the data collection system can be found in Refs. [10,11,12].

**Results and discussion.**—Only with the unique combination of the neutron converter, the RILIS, and the HRS, the selectivity needed for detailed  $\beta$ - and  $\gamma$ -spectroscopic measurements of very neutron-rich Cd isotopes was achieved. For time-dependent  $\gamma$ -ray singles and  $\gamma\gamma$ -coincidence spectroscopy, up to four large HPGe detectors were positioned in close geometry to the beam spot at the Moving Tape Collector (MTC). For  $\beta\gamma$  spectroscopy, the detector face-on to the MTC was replaced by a  $\Delta E$ - $E$   $\beta$  telescope. Altogether 20 new  $\gamma$  lines of the  $^{130}\text{Cd}$   $\beta$  decay and their coincidence relationships have been identified. An additional 315 keV transition belongs to the  $\beta dn$  decay of  $^{130}\text{Cd}$  ( $P_n = 3.6\%$  [6,13]) into the mass chain ( $A - 1$ ) = 129 and represents the well known  $1/2^+ \rightarrow 3/2^+$  ground-state transition in  $^{129}\text{Sn}$  [14].

Figure 1 shows the low-energy part of the  $^{130}\text{Cd}$ -decay scheme, in which eight  $\gamma$  transitions were included. For determining the respective log ft values, we have used our experimental  $Q_\beta$  value (see Fig. 2). Five clean transitions at 451, 1171, 1669, 1732, and 2120 keV could be combined with two  $\gamma$  lines at 389 and 950 keV, which are doublets

with strong  $^{130}\text{In}$  transitions, to establish a  $1^+$  level and its decay into the  $1^-$  ground state.

Recently, Hellström *et al.* [16] reported a  $\gamma$  line at 389 keV with a lifetime of  $<10 \mu\text{s}$ , which is associated with the decay of a previously unreported “ $\mu\text{s}$  isomer” in  $^{130}\text{In}$ . The existence of this level is confirmed by our data within a 1732–389 keV cascade, leading to the establishment of  $J^\pi = (3^+)$  for this isomer.

The  $\beta$  feedings of the levels at 1171, 1669, and 2586 keV suggest nonunique first-forbidden (ff) transitions, hence leading to tentative spin assignments of  $J^\pi = 0^-$  or  $1^-$ . Because of the direct production of surface-ionized In, the ground-state feeding could not be determined experimentally and was deduced from the Gross theory [17]. The log ft values for a cluster of seven levels above 4.4 MeV (not included in Fig. 1) clearly suggest GT feeding. These levels have a total  $\beta$  feeding of  $\approx 3.5\%$  and are, according to our quasiparticle random-phase approximation (QRPA) calculations, of  $[\pi g_{9/2} \otimes \nu g_{7/2}]$  4QP nature.

It becomes immediately evident that the major surprise of our results is the rather high excitation energy of 2120 keV for the  $[\pi g_{9/2} \otimes \nu g_{7/2}]$  2QP  $1^+$  state, populated by GT decay with a log ft  $\approx 4.1$ . The position of this level in  $^{130}\text{In}$  is determined by the strength of the proton-neutron interaction between the spin-orbit partners  $\pi g_{9/2}$  and  $\nu g_{7/2}$  relative to the  $\pi g_{9/2}$  and  $\nu h_{11/2}$  orbitals, as well as the difference between the position of the  $\nu h_{11/2}$  and the  $\nu g_{7/2}$  orbitals. In a recent large-scale shell-model calculation with the code ANTOINE, Martinez-Pinedo and Langanke [8] predicted this  $1^+$  level to lie at 1555 keV.

We have carried out calculations in the  $\pi\nu$  formalism with the shell-model code OXBASH [18]. The model space is that of a closed shell for  $^{132}\text{Sn}$  with single-particle energies taken from the experimental energies of  $^{131}\text{Sn}$ ,  $^{129}\text{Sn}$ , and Hartree-Fock calculations [19]. The residual

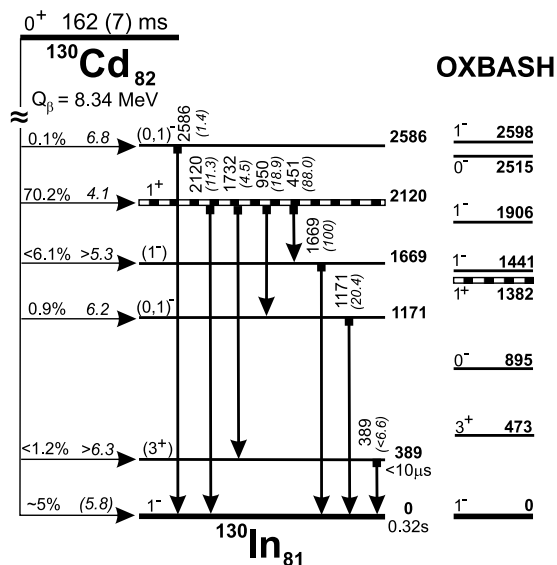


FIG. 1. Partial decay scheme of  $^{130}\text{Cd}$ , in comparison with predictions of low-lying  $1^+$ ,  $3^+$ ,  $0^-$ , and  $1^-$  levels in  $^{130}\text{In}$  from shell-model calculations using the code OXBASH. For further details, see the text.

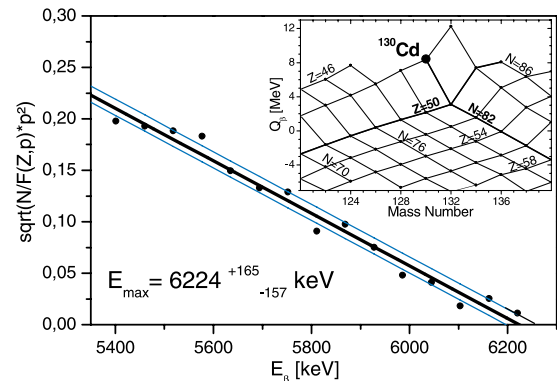


FIG. 2 (color online). Fermi-Kurie plot of  $^{130}\text{Cd}$ . The inset shows a “Way-Wood” diagram for even-even nuclides in the  $^{132}\text{Sn}$  region, including our new experimental value for  $^{130}\text{Cd}$  and the recent extrapolation for  $^{132}\text{Cd}$  of Audi *et al.* [15]. For discussion, see text.

two-body interaction is obtained starting with a  $G$  matrix derived from the charge-dependent (CD-Bonn) nucleon-nucleon interaction [20]. The harmonic oscillator basis was employed for the single-particle radial wave functions with an oscillator energy of  $\hbar\omega = 7.87$  MeV. The calculated spectrum for levels in  $^{130}\text{In}$  populated by GT and nonunique ff decay is shown in Fig. 1. The most striking feature is the fact that the energy of the calculated  $1^+$  state at 1.38 MeV is 0.74 MeV lower than the experimental value. The key two-body matrix element (TBME) of  $\langle 0g_{9/2}, 0g_{7/2}, 1^+ | V_{pn} | 0g_{9/2}, 0g_{7/2}, 1^+ \rangle = -2.8$  MeV is the largest  $\pi\nu$  TBME in the model space. To give better agreement with the experiment, we would need to change this TBME to  $\approx -2.0$  MeV, but the reason for this change is not understood. However, the calculations for nuclei such as  $^{130}\text{Sn}$ ,  $^{134}\text{Sn}$ , and  $^{134}\text{Te}$  agree with the experiment within  $\approx 100$  keV. All of these are associated with a  $T = 1$  Hamiltonian. Thus the problem must be connected with the  $\pi\nu$  or the  $T = 0$  Hamiltonian.

In order to obtain a physically consistent picture of all aspects of  $^{130}\text{Cd}$   $\beta$  decay, in addition to the  $T_{1/2}$ , the  $E^{1+}$  and its  $\beta$  feeding, we also need the GT-decay energy, which involves a knowledge of the  $Q_\beta$  value, to calculate the log ft value for this level. Therefore, in a second experiment we have measured  $\beta$  spectra in coincidence with the above  $\gamma$  lines. Figure 2 shows the resulting Fermi-Kurie plot for the sum of all five  $\beta\gamma$  gates depopulating the  $1^+$  level at 2120 keV.

The energy calibration was done via known  $Q_\beta$  values of  $^{92}\text{Rb}$ ,  $^{126}\text{In}$ ,  $^{130}\text{In}$  and their isomers. From the  $x$ -axis intercept of the Fermi-Kurie fit for  $^{130}\text{Cd}$ , a  $\beta$ -end point energy of 6224 keV was derived with a correlation coefficient  $R = 0.99$ , which led to an experimental  $Q_\beta$  value of  $(8344^{+165}_{-157})$  keV. In the inset of Fig. 2, we show a Way-Wood diagram for  $Q_\beta$  values of even-even isotopes in the  $^{132}\text{Sn}$  region, including our new value for  $^{130}\text{Cd}$  and the recent extrapolation for  $^{132}\text{Cd}$  [15]. From the slopes and distances of the respective isotopic and isotonic chains, the  $Z = 50$  and  $N = 82$  shell closures are clearly visible, as well as the different behavior of the  $Z = 48$  Cd and the  $Z = 52$  Te isotopes relative to the proton-magic Sn.

Comparing our experimental  $Q_\beta$  value for  $^{130}\text{Cd}$  with theoretical predictions, we find good agreement with the short-range extrapolation of  $8.5 \pm 0.4$  MeV from the Audi and Wapstra mass evaluation [21]. However, we recognize, that our value is considerably higher than the predictions of global mass models with strong neutron shell closures far from stability, such as the finite-range droplet model (FRDM) (7.43 MeV) [22], the extended Thomas-Fermi with Strutinsky integral (ETFSI-1) (7.86) [23], and the Duflo-Zuker mass formula (7.56 MeV) [24]. More recent mass models, which include the phenomenon of “shell quenching” at  $N = 82$ , turn out to be in much better agreement with our experimental value, e.g., the Hartree-Fock-Bogoliubov Skyrme force  $P$  (HFB-SkP) (8.93 MeV) [25] and the ETFSI- $Q$  (8.30 MeV) [26].

Surprisingly, the most recent microscopic HF mass models [27,28], which also should contain “quenching” in a self-consistent way, predict low  $Q_\beta$  values of 7.00 and 7.64 MeV, respectively.

Based on the so far known experimental log ft values  $\approx 4.1$ – $4.5$  for the  $[\pi g_{9/2} \otimes \nu g_{7/2}]$  configuration in the  $^{132}\text{Sn}$  region [14] and our rather high  $E^{1+}$  of 2.12 MeV, a GT-decay energy of  $(Q_\beta - E^{1+}) \approx 6.1$  MeV is required in order to obtain a physically reasonable picture for all aspects of  $^{130}\text{Cd}$   $\beta$  decay. Thus, we can exclude mass models with “low”  $Q_\beta$  predictions for  $^{130}\text{Cd}$ , because with a GT-decay energy of  $\approx 5.4$  MeV they would lead to unreasonably low log ft values of  $\approx 3.8$  for the  $1^+$  level. On the other hand,  $N = 82$  shell quenching seems to be required for a “high”  $Q_\beta$  value and a log ft  $\approx 4.1$ , as in our experiment.

However, it is not possible to draw wide-ranging conclusions from a single isobaric mass difference. Hence, we also want to consider experimental and theoretical mass differences of isotopic chains in the  $^{132}\text{Sn}$  region. In Fig. 3 we show two mass difference plots for  $Z = 50$  Sn and  $Z = 48$  Cd isotopes, normalized to the “unquenched” macroscopic-microscopic FRDM model predictions. This model still has the best overall predictive power for the whole ensemble of radioactive nuclides

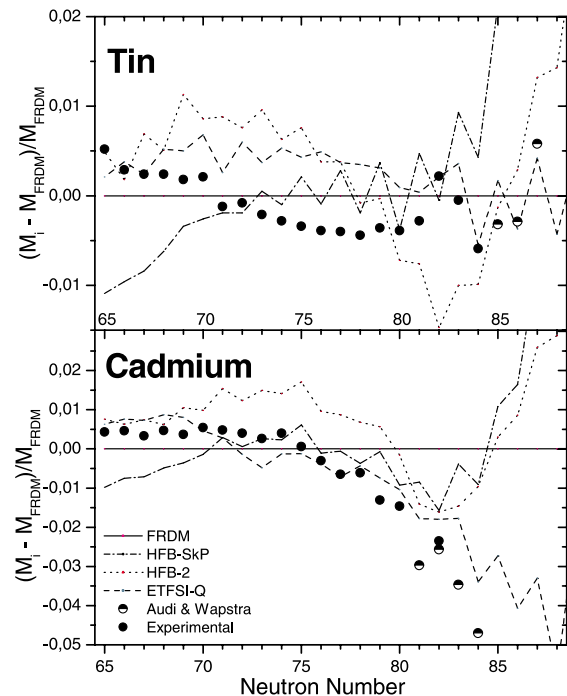


FIG. 3 (color online). Comparison of normalized mass deviations of  $^{50}\text{Sn}$  and  $^{48}\text{Cd}$  isotopes from model predictions with “shell quenching” [25,26,28], experimental values, and very recent short-range extrapolations for  $^{135-137}\text{Sn}$  and  $^{129-132}\text{Cd}$  [15,21] relative to the “unquenched” FRDM [22]. The deviation to our experimental value of  $^{130}\text{Cd}$  corresponds to a mass difference of 1.57 MeV.

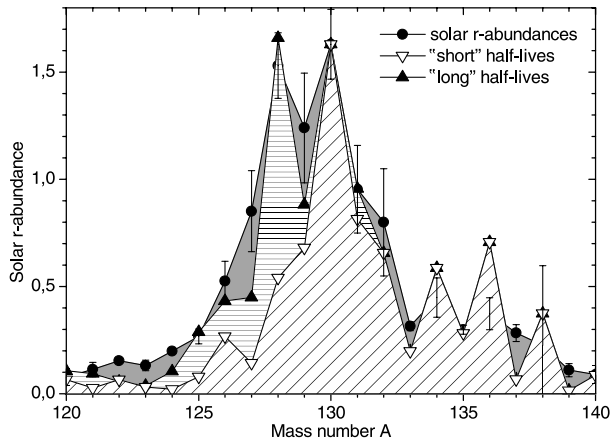


FIG. 4. Comparison of the solar system  $r$ -process abundances ( $N_{r,\odot}$ ) in the  $A \approx 130$  peak region with model predictions. Within the classical “waiting-point” concept, the “longer” half-lives concluded from our new nuclear-structure information result in a better reproduction of the rising wing of the solar  $r$ -abundance ( $N_{r,\odot}$ ) peak.

[29]. As can be seen from this figure, there is a significant change in the *trend* of experimental and theoretical mass differences between the isotones of these two elements. Negative values reflect less binding energy (higher  $Q_\beta$  value) compared to the FRDM prediction.

For the Cd chain, a much better agreement with the experimental data is obtained with quenched mass models than with the FRDM or other unquenched models. If we take the most recent Audi *et al.* [15] mass predictions into account, only the ETFSI- $Q$  follows the continuing decline. The overall behavior of the HFB-2 model is surprisingly poor, and the slopes for the microscopic quenched mass models strongly diverge beyond  $N = 82$ . It is obvious from this figure that there is a need for *experimental* masses of the Cd isotopes  $^{129}\text{Cd}$ ,  $^{131}\text{Cd}$ , and  $^{132}\text{Cd}$  to confirm the occurring downward trend. Nevertheless, we believe that our experimental confirmation of a high  $Q_\beta$  value for  $^{130}\text{Cd}$  is a direct signature of an  $N = 82$  shell quenching below  $^{132}\text{Sn}$ .

*Implications for the  $r$  process.*—As a consequence of the required change of the TBME for  $^{130}\text{Cd}$  decay (resulting in the observed energy shift of the  $E^{1+}$  in  $^{130}\text{In}$ ), the  $\beta$ -decay half-lives of the so far unknown  $N = 82$  waiting-point nuclei  $^{128}\text{Pd}$  to  $^{122}\text{Zr}$  will become *longer* than those predicted by recent large-scale shell models [7,8,18]. As shown in Fig. 4, this leads in dynamical  $r$ -process abundance calculations to a better reproduction of the rising wing of the  $A \approx 130$   $N_{r,\odot}$  peak compared to calculations with the previous “short” shell-model half-lives. For this plot, only the half-lives for  $A < 131$  were replaced by experimental data and new model predic-

tions, and then normalized to  $A = 130$ . The direct consequence for astrophysics is a better understanding of the  $r$ -process matter flow through this “bottleneck” region, which, to a large extent, also determines the total duration of a *classical*  $r$  process [30].

This work was supported by the German BMBF, the Schweizer Nationalfond, the U.S. DOE, and NSF. B. A. B. acknowledges support from NSF Grant No. PHY-0244453.

\*Electronic address: kl.kratz@uni-mainz.de

- [1] E. M. Burbidge *et al.*, Rev. Mod. Phys. **29**, 547 (1957).
- [2] C. D. Coryell, J. Chem. Educ. **38**, 67 (1961).
- [3] K.-L. Kratz *et al.*, Z. Phys. A **325**, 489 (1986).
- [4] K.-L. Kratz *et al.*, J. Phys. G **14**, 331 (1988).
- [5] B. Pfeiffer *et al.*, Nucl. Phys. **A693**, 282 (2001).
- [6] M. Hannawald *et al.*, Nucl. Phys. **A688**, 578c (2001).
- [7] J. Engel *et al.*, Phys. Rev. C **60**, 014302 (1999).
- [8] G. Martinez-Pinedo and K. Langanke, Phys. Rev. Lett. **83**, 4502 (1999).
- [9] J. A. Nolen *et al.*, in *Heavy Ion Acceleration Technology*, edited by K. W. Shepard, AIP Conf. Proc. No. 473 (AIP, New York, 1999), p. 477.
- [10] M. Hannawald *et al.*, Phys. Rev. C **62**, 054301 (2000).
- [11] I. Dillmann, Diploma Thesis, Universität Mainz, 2002.
- [12] U. Köster *et al.*, Nucl. Instrum. Methods Phys. Res., Sect. B **204**, 347 (2003).
- [13] B. Pfeiffer *et al.*, Prog. Nucl. Energy **41**, 39 (2002).
- [14] R. B. Firestone *et al.*, *Table of Isotopes* (Wiley, New York, 1996), 8th ed.
- [15] Atomic Mass Data Center, Program PC-NUCLEUS, <http://csnwww.in2p3.fr/AMDC/web/> (2003).
- [16] M. Hellström *et al.*, *Proceedings of the XXXI International Workshop on Gross Properties of Nuclei and Nuclear Excitations, Hirschegg, Austria, 2003* (GSI Report, ISSN 0720-8715, 2003) p. 72.
- [17] K. Takahashi *et al.*, At. Data Nucl. Data Tables **12**, 101 (1973).
- [18] B. A. Brown *et al.*, Nucl. Phys. **A719**, 177c (2003).
- [19] B. A. Brown, Phys. Rev. C **58**, 220 (1998).
- [20] R. Machleidt *et al.*, Phys. Rev. C **53**, R1483 (1996).
- [21] G. Audi *et al.*, Nucl. Phys. **A624**, 1 (1997).
- [22] P. Möller *et al.*, At. Data Nucl. Data Tables **59**, 185 (1995).
- [23] Y. Aboussir *et al.*, At. Data Nucl. Data Tables **61**, 127 (1995).
- [24] J. Duflo and A. P. Zuker, Phys. Rev. C **52**, R23 (1995).
- [25] J. Dobaczewski *et al.*, Phys. Rev. C **53**, 2809 (1996).
- [26] J. M. Pearson *et al.*, Phys. Lett. B **387**, 455 (1996).
- [27] S. Goriely *et al.*, At. Data Nucl. Data Tables **77**, 311 (2001).
- [28] M. Samyn *et al.*, Phys. Rev. C **66**, 024326 (2002).
- [29] D. Lunney *et al.*, Rev. Mod. Phys. (to be published).
- [30] P. Möller, B. Pfeiffer, and K.-L. Kratz, Phys. Rev. C **67**, 055802 (2003).